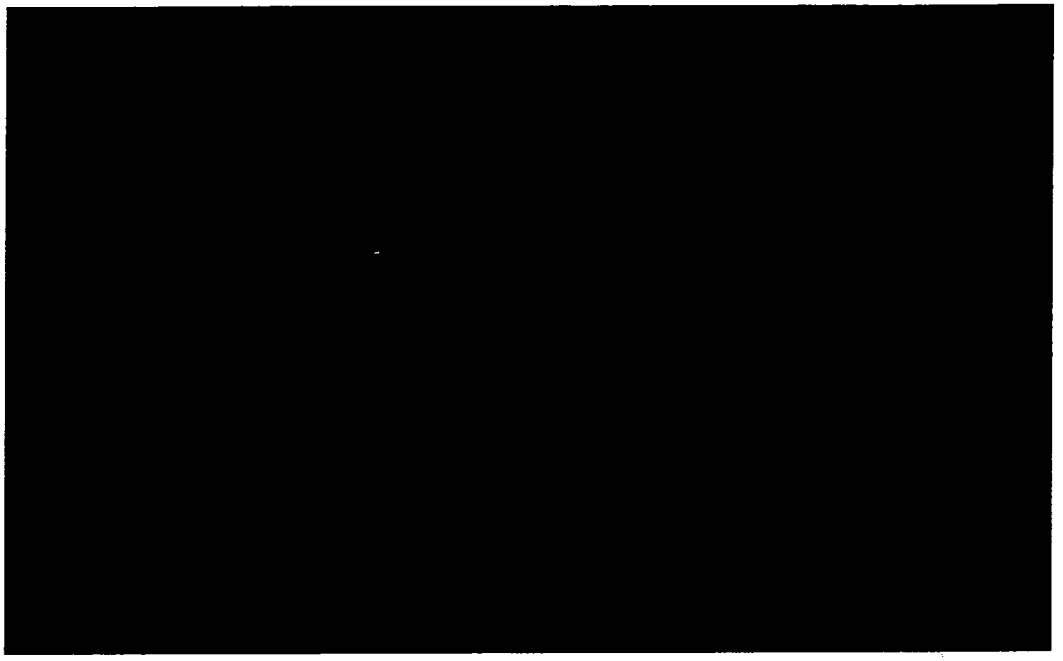

Figure 9.
The effect of osteopontin on chondrocyte transglutaminase activity. Chondrocytes were incubated with various doses of milk osteopontin for 48 hours. Transglutaminase activity was measured in the cell layer using a standard radiometric assay, and was corrected for protein in the sample. Osteopontin significantly increased transglutaminase activity at all concentrations tested ($n= 4$, $p < 0.01$).

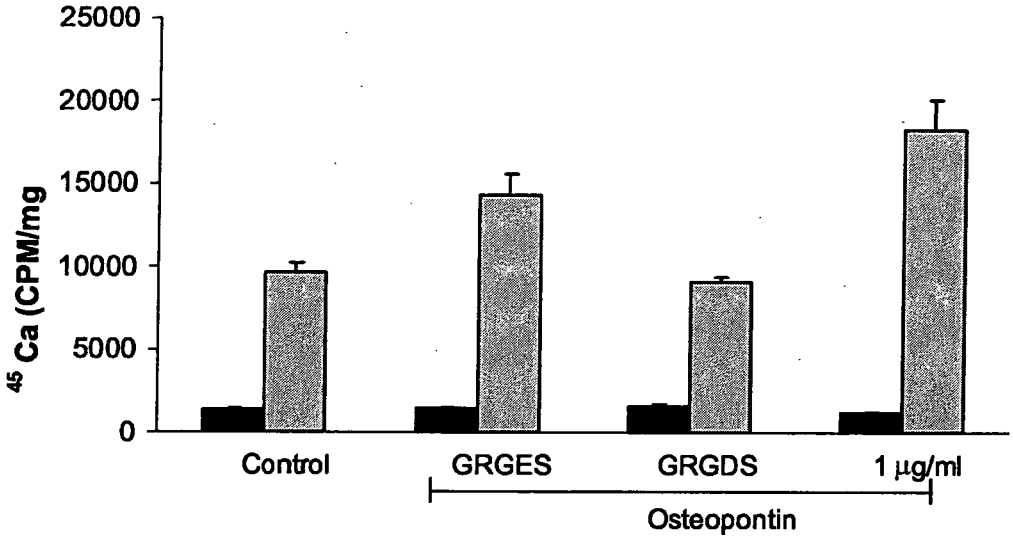

Figure 10.

The effect of an integrin antagonist on osteopontin-induced stimulation of CPPD crystal formation. Chondrocytes were incubated with no additives (Control), 40 µM inactive peptide control (GRGES), 40 µM integrin antagonist (GRGDS) or 1 µg/ml milk osteopontin in the presence of ^{45}Ca and with or without 1 mM ATP. After 48 hours, media were removed, and cell layers were thoroughly washed. ^{45}Ca levels in the cell layer were measured with liquid scintigraphy and corrected for cell protein. Black bars represent results with no ATP. Grey bars represent results with ATP. Values are means ± standard deviations (n=12). Over multiple experiments, the GRGES peptide had no statistically significant effect on osteopontin-induced CPPD crystal formation at doses of 5-40 µM (p=.06), while the GRGDS peptide significantly reduced osteopontin-induced CPPD crystal formation ($p \leq .001$)

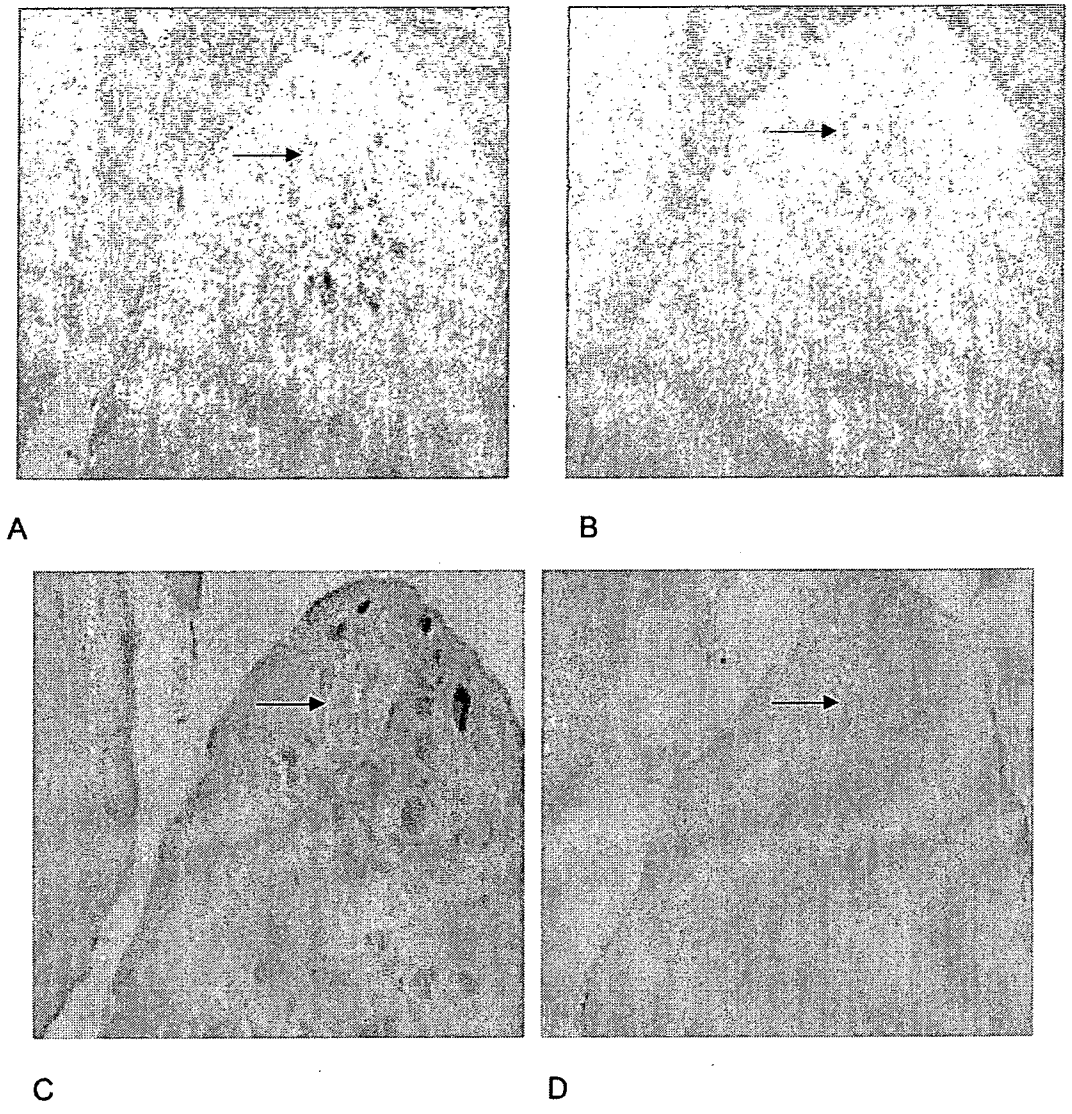

Figure 11.
Distribution of osteopontin and transglutaminase crosslinks in human CPPD-diseased articular cartilage. Immunohistochemistry was performed with anti-osteopontin antibody (Panel A), non-immune rabbit serum (Panel B), or antibody to the transglutaminase specific crosslink (Panel C), or non-immune mouse serum (Panel D) in human CPPD diseased articular cartilage. Arrows demonstrate CPPD crystals in the tissue slices. The presence of immunoreactive protein is demonstrated by brown staining.

TABLE 1

The effect of osteopontin on pyrophosphate levels in chondrocyte cultures.

Osteopontin (μg/ml)	Pyrophosphate (μM)**
0	2.6± 0.2
0.1	3.1± 0.6
1	3.3± 0.7
10	2.3± 0.1
25	2.3± 0.01

** Various concentrations of milk osteopontin were added to chondrocyte cultures. After 48 hours, pyrophosphate levels were measured in conditioned media. Values represent means ± standard deviations (n=6). Osteopontin did not significantly affect pyrophosphate levels at any concentration (p= 0.1).

ELSEVIER

Bone 40 (2007) 876–887

BONE

www.elsevier.com/locate/bone

Effects of aromatase inhibitors on human osteoblast and osteoblast-like cells: A possible androgenic bone protective effects induced by exemestane

Yasuhiro Miki [a], Takashi Suzuki [a], Masahito Hatori [b], Katsuhide Igarashi [c], Ken-ich Aisaki [c], Jun Kanno [c], Yasuhiro Nakamura [a], Miwa Uzuki [d], Takashi Sawai [c], Hironobu Sasano [a,*]

[a] *Department of Pathology, Tohoku University Graduate School of Medicine, 2-1 Seiryo-machi, Aoba-ku, Sendai, Miyagi, 980-8575, Japan*
[b] *Department of Orthopedic Surgery, Tohoku University Graduate School of Medicine, Sendai, Japan*
[c] *Division of Toxicology, National Institute of Health Sciences, Biological Safety Research Center, Setagaya, Tokyo, Japan*
[d] *Department of Pathology, Iwate Medical College, Morioka, Japan*

Received 21 April 2006; revised 6 November 2006; accepted 14 November 2006
Available online 28 December 2006

Abstract

Effects of aromatase inhibitors (AIs) on the human skeletal system due to systemic estrogen depletion are becoming clinically important due to their increasing use as an adjuvant therapy in postmenopausal women with breast cancer. However, possible effects of AIs on human bone cells have remained largely unknown. We therefore studied effects of AIs including the steroidal AI, exemestane (EXE), and non-steroidal AIs, Aromatase Inhibitor I (AI-I) and aminoglutethimide (AGM), on a human osteoblast. We employed a human osteoblast cell line, hFOB, which maintains relatively physiological status of estrogen and androgen pathways of human osteoblasts, i.e., expression of aromatase, androgen receptor (AR), and estrogen receptor (ER) β. We also employed osteoblast-like cell lines, Saos-2 and MG-63 which expressed aromatase, AR, and ERα/β in order to further evaluate the mechanisms of effects of AIs on osteoblasts. There was a significant increment in the number of the cells following 72 h treatment with EXE in hFOB and Saos-2 but not in MG-63, in which the level of AR mRNA was lower than that in hFOB and Saos-2. Alkaline phosphatase activity was also increased by EXE treatment in hFOB and Saos-2. Pretreatment with the AR blocker, flutamide, partially inhibited the effect of EXE. AI-I exerted no effects on osteoblast cell proliferation and AGM diminished the number of the cells. hFOB converted androstenedione into E2 and testosterone (TST). Both EXE and AI-I decreased E2 level and increased TST level. In a microarray analysis, gene profile patterns following treatment with EXE demonstrated similar patterns as with DHT but not with E2 treatment. The genes induced by EXE treatment were related to cell proliferation, differentiation which includes genes encoding cytoskeleton proteins. We also examined the expression levels of these genes using quantitative RT-PCR in hFOB and Saos-2 treated with EXE and DHT and with/without flutamide. HOXD11 gene known as bone morphogenesis factor and osteoblast growth-related genes were induced by EXE treatment as well as DHT treatment in both hFOB and Saos-2. These results indicated that the steroidal aromatase inhibitor, EXE, stimulated hFOB cell proliferation via both AR dependent and independent pathways.

Keywords: Osteoblast; Aromatase inhibitor; Androgen; Estrogen; Exemestane

Introduction

Results in various epidemiological or clinical studies demonstrated that estrogens play important protective roles in human skeletal as well as cardiovascular systems, and estrogen deficiency resulted in accelerating the development of osteoporosis in postmenopausal women [1–3]. In breast cancer of postmenopausal women, hormone therapies without any clinically deleterious effects due to estrogen deficiency on bone metabolism as well as lipid metabolisms are preferable. Estrogen deficiency has been generally detected in the patients with breast cancer following chemotherapy induced ovarian failure, gonadotropin analogue, and aromatase inhibitors (AIs) therapy [4]. Aromatase is the pivotal enzyme of *in situ* or intratumoral estrogen biosynthesis in postmenopausal breast cancer patients, and catalyzes the conversion from androgens into estrogens (Fig. 1A). AIs therefore play an important role in

* Corresponding author. Fax: +81 22 273 5976.
E-mail address: hsasano@patholo2.med.tohoku.ac.jp (H. Sasano).

8756-3282/$ - see front matter © 2006 Elsevier Inc. All rights reserved.
doi:10.1016/j.bone.2006.11.029

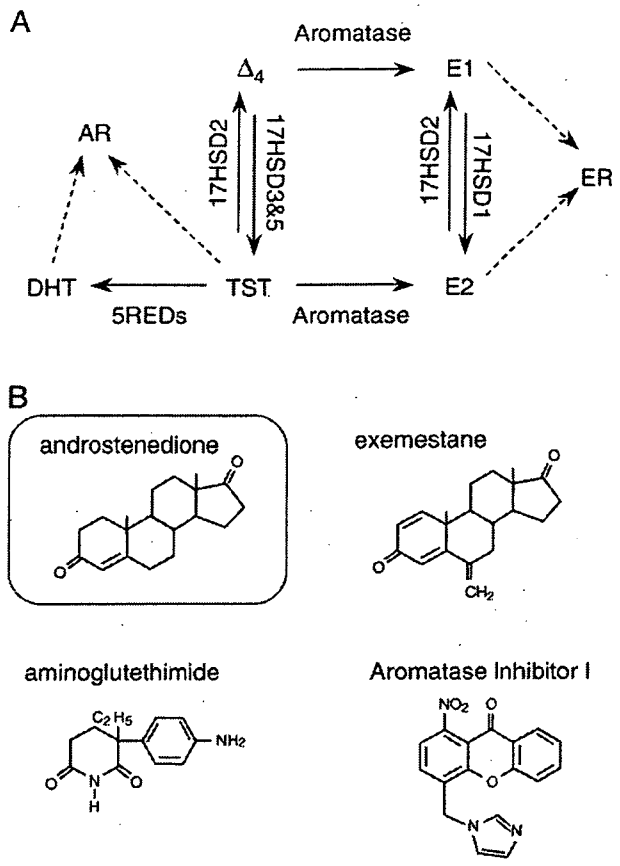

Fig. 1. (A) Summary of the pathway of estrogens and androgens production. Aromatase catalyzes the change from androstenedione (Δ4) and testosterone (TST) into estrone (E1) and estradiol (E2), respectively. 17HSD, 17β-hydroxysteroid dehydrogenase; 5REDs, 5α-reductase types 1 and 2; AR, androgen receptor; DHT, 5α-dihydrotestosterone; ER, estrogen receptor. (B) Structure of aromatase inhibitors used in this study. Androstenedione is a natural substrate of aromatase. Steroidal aromatase inhibitor, exemestane has an androstenedione-like structure.

clinical management of both primary and advanced breast cancer in postmenopausal women [5]. AIs are classified into two classes according to their modes of action. Type I AIs are steroidal inhibitions and one of them, exemestane (EXE) inhibits aromatase irreversibly and has an androstenedione (Δ_4)-like structure (Fig. 1B) [5–7]. Type II AIs are non-steroidal inhibitions and include aminoglutethimide (AGM), anastrozole, and letrozole [5].

Results of *in vivo* study using ovariectomized (OVX) rats demonstrated that EXE and its principal metabolite form, 17-hydroexemestane (17H-EXE) but not letrozole significantly prevented bone loss in OVX rats [8,9]. EXE and its principal metabolite, 17H-EXE, are structurally related to Δ_4 and bind to androgen receptor (AR) with relatively low affinity compared to 5α-dihydrotestosterone (DHT) [7]. These finding suggest that EXE may demonstrate protective effects toward bone tissues through its androgenic actions. However, detailed mechanisms of effects of EXE or androgen itself on human bone cells have remained largely unknown.

Various studies using human or animal bone tissues [10,11] and osteoblast cell culture using osteosarcoma cells [12,13] demonstrated that aromatase mRNA or protein was detected in osteoblast cells, which play an important role in bone remodeling. Therefore, in this study, we focused on effects of EXE in human osteoblast in an initial attempt to evaluate the effects of these AIs (summarized in Table 1 and Fig. 1B) [5–7,14], including AGM, EXE, and an experimental compound for inhibition of aromatase, Aromatase Inhibitor I (AI-I) [14] on human osteoblast and osteoblast-like cell lines. In our present study, we employed normal human cell line, hFOB, which maintains native characteristics of sex steroid hormone pathway of human osteoblasts, i.e., expression of AR, ERβ but not ERα, and aromatase. We also employed other osteoblast-like cell lines, Saos-2 and MG-63 which expressed ERα as well as ERβ in order to further study the mechanisms of effects of AI on human osteoblasts. We first examined the effects of estradiol (E2), DHT, progesterone (Prg), and AIs described above on cell proliferation of these cell lines, because the status of cell proliferation is important in the maintenance of homeostasis of bone tissue [15]. In addition, the effects of AIs on the conversion ratio of Δ_4 into E2 or testosterone (TST) in hFOB cultured medium were examined. We then screened E2, DHT, and EXE responsive genes using a microarray analysis in these cells, in order to further characterize the possible genomic effects of EXE on cell proliferation of osteoblasts. In this microarray analysis, hFOB was employed in order to examine the effects of E2, DHT, and EXE on native status of human osteoblasts but not on pathological status of osteoblasts such as osteosarcomas.

Materials and methods

Chemicals

Exemestane (EXE; FCE24304; 6-methyleneandrosta-1,4-diene-3,17-dione) and 17-hydroexemestane (17H-EXE; FCE25071; 6-methyleneandrosta-1,4-diene-17β-ol-3-one) were obtained from Pfizer, Inc. (MI, USA). Aminoglutethimide (AGM) and Aromatase Inhibitor I [AI-I; 4-(Imidazolylmethyl)-1-nitro-9*H*-9-xanthenone] were obtained from Sigma-Aldrich Co. (MO, USA) and EMD Biosciences, Inc. (CA, USA), respectively. Estradiol (E2), progesterone (Prg), and RU38,486 (RU; mifepristone), spironolactone were obtained from Sigma-Aldrich. ICI 182,780 (ICI; fulvestrant) and hydroxyflutamide (OHF) were obtained from Tocris Cookson Inc. (MO, USA) and Toronto Research Chemicals, Inc. (Ontario, Canada), respectively. 5α-dihydrotestosterone (DHT) was obtained from Wako Pure Chemical industries, Ltd. (Osaka, Japan).

Table 1
Aromatase inhibitors used in this study

	Aminoglutethimide	Exemestane	Aromatase inhibitor I
Trademark[a]	Cytadren®	Aromasin®	–
Type[b]	Type II	Type I	Type II
Generation	First	Third	–
IC50 (nM)[c]	3000	50	40

[a] Cytadren® is trademark of Novartis Pharmaceutical Corporation. Aromasin® is trademark of Pfizer Inc. Aromatase Inhibitor I is non-clinical compound of Calbiochem®.

[b] Type I is steroidal compound. Type II is a non-steroidal compound.

[c] Refs, Aminoglutethimide and Exemestane are Miller et al. [5]; Aromatase Inhibitor I is Recanatini et al. [14].

These materials were dissolved in pure ethanol (Wako Pure Chemical industries) and serially diluted (final concentrations: 10^{-12} M to 10^{-5} M), respectively. AGM was dissolved in DMSO (Wako Pure Chemical industries). The final concentration of ethanol and DMSO used in this study did not exceed 0.05%.

Osteoblast cell and osteoblast-like cell lines and culture conditions

Human normal osteoblast cell, hFOB 1.19 cell line (CRL-11372) was obtained from American Type Culture Collection (VA, USA). hFOB 1.19 cell was cultured according to the protocol previously described [16]. The cell line was maintained in a mixture of Dulbecco's Modified Eagle Medium and Ham's F12 medium (1:1) without phenol red (Invitrogen Corporation, CA, USA) supplemented with 10% fetal bovine serum (FBS; JRH Biosciences, KS, USA) and 50 mg/mL G 418 sulfate (EMD Biosciences). Human osteosarcoma cell lines Saos-2 and MG-63 were provided from the Cell Resource Center for Biomedical Research, Tohoku University (Sendai, Japan) and were maintained in a RPMI-1640 (Sigma-Aldrich) with 10% FBS. These cells were pre-incubated for 24 h with FBS-free medium prior to examination in order to remove exo-/endogenous steroid hormones from the culture medium and study the effects of various compounds in the absence of steroids and also to synchronize the cell cycle. Different concentrations of test compounds were added, and the assay was terminated after 3 or 5 days by removing the medium from wells. Steroid blockers were added simultaneously.

Characteristics of hFOB, Saos-2, and MG-63

Expressions of relevant steroid receptors, i.e., ERα, ERβ, and AR were determined using quantitative RT-PCR methods in hFOB, Saos-2, and MG-63 cell lines. mRNA transcripts of steroid synthesis/metabolite enzymes, aromatase, 17β-hydroxysteroid dehydrogenase (17β-HSD) types 1, 2, 3, 4, and 5, and 5α-reductase (5α-Red) types 1 and 2 were all evaluated using RT-PCR methods. The details of quantitative RT-PCR including primer sets employed were previously described in detail [17,18]. Positive controls for these receptors and enzymes were cell lines of human breast cancer, T-47D, and human prostate cancer, LNCaP obtained from Cell Resource Center for Biomedical Research, Tohoku University (Sendai, Japan). Alkaline phosphatase (ALP), an osteoblast-specific marker, was also studied using RT-PCR for characterization of these cell lines.

Estradiol and testosterone production assay

hFOB cells were plated in 10 mm dishes at a density of 10^6 viable cells and cultured for 48 h. Then media were changed to FBS-free medium, and hFOB cells were incubated with 10^{-7} M androstenedione (Δ_4; Sigma-Aldrich) in the presence or absence of EXE or AI-I (10^{-7} M). The media were then collected after 24 h, and E2 and TST were measured by solid-phase radioimmunoassay. Radioimmunoassay was performed in SRL Inc. (Tokyo, Japan) using DPC estradiol kit and DPC total testosterone kit (Diagnostic Products Corporation, LA, USA). In addition, we confirmed that the concentrations of E2 and TST were under the detection limits (E2, 5 pg/mL; TST, 30 pg/mL) in the serum- and phenol red-free medium.

Cell proliferation assay

hFOB, Saos-2, and MG-63 cells were treated with steroids and test compounds for 24, 48, and 72 h, when specimens were harvested and evaluated for cell proliferation using the WST-8 method (Cell Counting Kit-8; Dojindo Inc., Kumamoto, Japan) [18]. Optical densities (OD, 450 nm) were evaluated using a SpectraMax 190 microplate reader (Molecular Devices, Corp., CA, USA) and Softmax Pro 4.3 microplate analysis software (Molecular Devices). The status of proliferation (%) was calculated according to the following equation: (cell OD value after test materials treated/vehicle control cell OD value) × 100.

Alkaline phosphatase activity assay

hFOB, Saos-2, and MG-63 cells were plated in 48 well plate at a density of 10^6 viable cells and cultured for 48 h. All cell lines were treated with 10^{-9} to 10^{-7} M exemestane for 72 h, when cells were lysed with 0.05% Triton X-100 (Wako Pure Chemical industries) and evaluated for alkaline phosphatase activity

Table 2
Primer sequences used in quantitative RT-PCR analysis

cDNA	GB#	Sequence	cDNA position	Size (bp)
MYBL2	NM_002466	Forward 5′-GTAACAGCCTCACGCCCAAGA-3′ Reverse 5′-TCCAATGTGTCCTGTTTGTTCCA-3′	1522–1615	94
OSTM1	NM_014028	Forward 5′-TTGAGAATAAGGCTGAACCTGGAAC-3′ Reverse 5′-TTACAGGCACTGTGTCACTGCAAG-3′	801–926	126
HOXD11[a]	NM_021192	Forward 5′-CAC TGT CCT TGG GTT TAA TG-3′ Reverse 5′-GGT AAA ATT GTA ACG GGA CG-3′	1091–1245	174
GPC2	NM_152742	Forward 5′-AGA AAT GTG GTC AGC GAA GC-3′ Reverse 5′-ACA CCT TCG CAC TGT TTT CC-3′	871-1183	313
ADCYAP1R1	NM_001118	Forward 5′-CAG CAA AAG GGA AAG ACT CG-3′ Reverse 5′-GAG CTG CTC TTG CTC AGG AT-3′	1351–1584	234
COL1A1	NM_000088	Forward 5′-GGT GGT GGT TAT GAC TTT GGT T-3′ Reverse 5′-CTT GGC TGG GAT GTT TTC AGG T-3′	3784–4092	309
SMAD1[a]	NM_005900	Forward 5′-GGT TCA CCT CAT AAT CCT-3′ Reverse 5′-CCT TTG TCA GTT CTC AAT C-3′	1779–1887	127
SMAD5[a]	NM_005903	Forward 5′-AGC TAA AGC CGT TGG ATA-3′ Reverse 5′-AGG CAC TAA TAC TGG AGG T-3′	668–768	119
RUNX2	NM_004348	Forward 5′-GTG GAC GAG GCA AGA GTT T-3′ Reverse 5′-TAC TGG GAT GAG GAA TGC G-3′	782–961	198
SPARC	NM_003118	Forward 5′-CCT GTA CAC TGG CAG TTC-3′ Reverse 5′-CCA GGG CGA TGT ACT TGT C-3′	793–937	163
ALP	NM_000478	Forward 5′-ACC ATT CCC ACG TCT TCA CA-3′ Reverse 5′-AGA CAT TCT CTC GTT CAC CGC C-3′	1379–1540	162
RPL13A	NM_012423	Forward 5′-CCT GGA GGA GAA GAG GAA AGA GA-3′ Reverse 5′-TTG AGG ACC TCT GTG TAT TTG TCA A-3′	487–612	126

GB#, GeneBank accession number.
All primer sets were designed using OLIGO Primer Analysis Software (TAKARA Bio Inc., Shiga, Japan).
[a] Forward and reverse primers were located in sama exon.

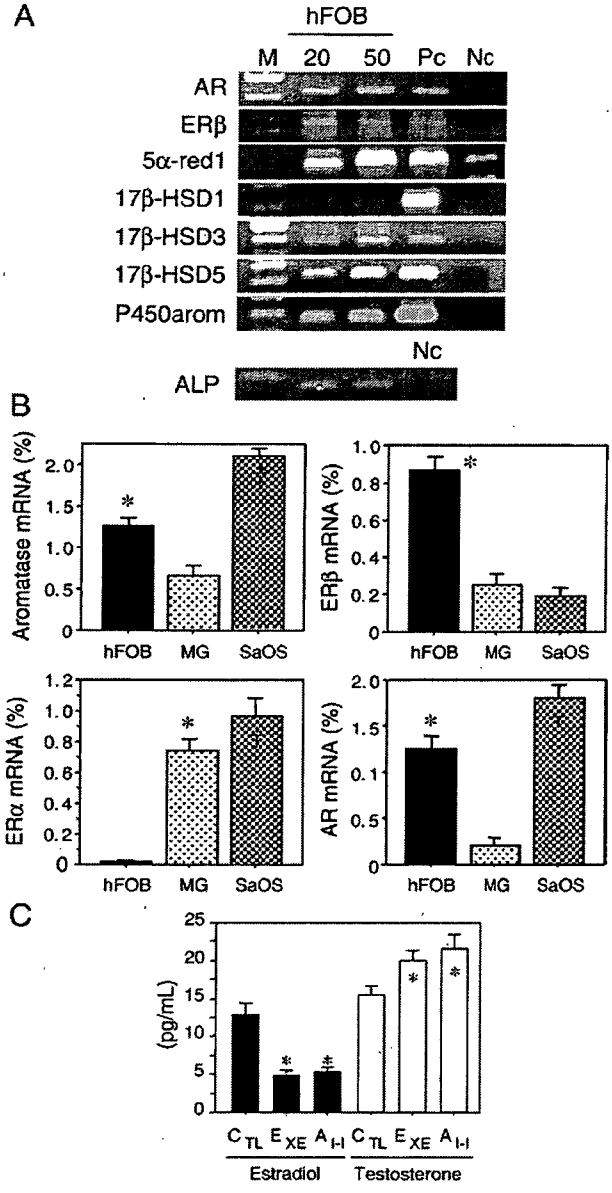

Fig. 2. (A) Results of RT-PCR analysis of steroid hormone receptors and steroid-related enzymes. Both 20 and 50 ng/μL cDNA of hFOB were used for PCR (ALP was 20 ng/μL alone). AR, androgen receptor; ER, estrogen receptor; 5α-red1, 5α-reductase type 1; 17β-HSD, 17β-hydroxysteroid dehydrogenase; P450 arom, aromatase; M, molecular marker; Pc, positive control; Nc, negative control. (B) Expression levels of aromatase, AR, ERα, and ERβ in hFOB, Saos-2, and MG-63. *$p<0.05$ vs. MG-63 (aromatase and AR), vs. MG-63 and vs. Saos-2 (ERβ), vs. hFOB (ERα); †$p<0.05$ vs. hFOB and MG-63 (aromatase and AR), vs. MG-63 and hFOB (ERα). (C) Estradiol and testosterone productions in hFOB cells. The data are expressed as the mean SD ($n=3$). *$p<0.05$ vs. control cells (CTL). EXE, 10^{-7} M exemestane; AI-I, 10^{-7} M aromatase inhibitor I.

using the *p*-nitrophenylphosphate method (LabAssay ALP; Wako Pure Chemical industries) [19]. Optical densities (OD, 405 nm) were evaluated using a SpectraMax 190 microplate reader (Molecular Devices) and Softmax Pro 4.3 microplate analysis software (Molecular Devices). ALP activity (units/μL)=(concentration of *p*-nitrophenol/15 min)×1 (dilution factor of sample). The ALP activities were presented as units/μL/10^6 cells. The ALP activity levels in each case were represented as a ratio of vehicle control (%).

Microarray analysis

The procedure was based on a previously reported study [20]. Cell lysates were prepared using RLT buffer (QIAGEN GmbH, Hilden, Germany). Total RNA was extracted using RNeasy Mini Kit (QIAGEN). First-strand cDNA was synthesized by incubating 5 μg of total RNA with 200 U SuperScript II reverse transcriptase (Invitrogen), 100 pmol T7-(dT)24 primer (Invitrogen). Ten units of T4 DNA polymerase (Invitrogen) were then added, and the dsDNA was mixed with T7 RNA polymerase (Invitrogen). The purified cRNA was fragmented at 300–500 bp as target solution. Hybridization was performed with the GeneChip Human Genome 133 ver. 2.0 (Affymetrix, Inc., CA, USA). The reacted arrays were then scanned as digital image files and scanned data were analyzed with GeneChip software (Affymetrix). Relative levels of gene expression were calculated by global normalization.

Data were subjected to hierarchical clustering analysis and visualization using the Cluster and TreeView programs (Stanford University) in order to generate tree structures based on the degree of similarity, as well as matrices comparing the levels of expression of individual genes in each sample [21].

Real-time PCR

Real-time PCR was carried out using the LightCycler System and the FastStart DNA Master SYBR Green I (Roche Diagnostics GmbH, Mannheim, Germany). The primer sequences used in this study are summarized in Table 2. An initial denaturing step of 95 °C for 10 min was followed by 35 cycles, respectively, at 95 °C for 10 min; 15 s annealing at 65 °C (ALP, COL1A1), 64 °C (MYBL2, OSTM1, RPL13A), 62 °C (SMAD1, SMAD5, SPARC, RUNX2), or 60 °C (HOXD11); and extension for 15 s at 72 °C. Negative control experiments included those lacking cDNA substrates to confirm the presence of exogenous contaminant DNA. No amplified products were detected under these conditions. The mRNA levels in each case were represented as a ratio of RPL13A (%) [22].

Immunohistochemistry of AR

Five non-pathological bone tissues were retrieved from surgical pathology files (two females and three males, 17 to 55 years old) of Department of Pathology, Tohoku University Hospital (Sendai, Japan).

Tissue sections were immunostained using a biotin-streptavidin method with Histofine kit (Nichirei Co. Ltd., Tokyo, Japan). The monoclonal antibody for AR (AR411) [23] was obtained from DakoCytomation (Kyoto, Japan). Experimental procedures employed in our present study have been previously described in detail [22,23]. The dilutions of primary AR antibody were 1:100. The antigen-antibody complex was then visualized with 3,3′-diaminobenzidine solution, and counterstained with hematoxylin. Prostate cancer was used as a positive control for AR. Normal mouse IgG was used as a negative control for immunostaining and no specific immunoreactivity was detected.

Statistical analysis

Results were expressed as mean±SD. Statistical analysis was performed with the StatView 5.0 J software (SAS Institute Inc., NC, USA). All data were analyzed by analysis of variance (ANOVA) followed by post hoc Bonferroni/Dunnett multiple comparison test. A *p*-value<0.05 was considered to indicate statistical significance.

Results

Characteristics of hFOB, MG-63, and Saos-2 cell line

Characteristics of osteoblast and osteoblast-like cell lines are summarized in Figs. 2A and B. hFOB cells expressed mRNA transcripts of AR and ERβ. Relatively low level of ERα mRNA transcript was detected in hFOB cells. Aromatase, 17β-HSD type 1, 3, and 5, and 5α-Red types 1 and 2 mRNA transcripts were all detected in hFOB cells by

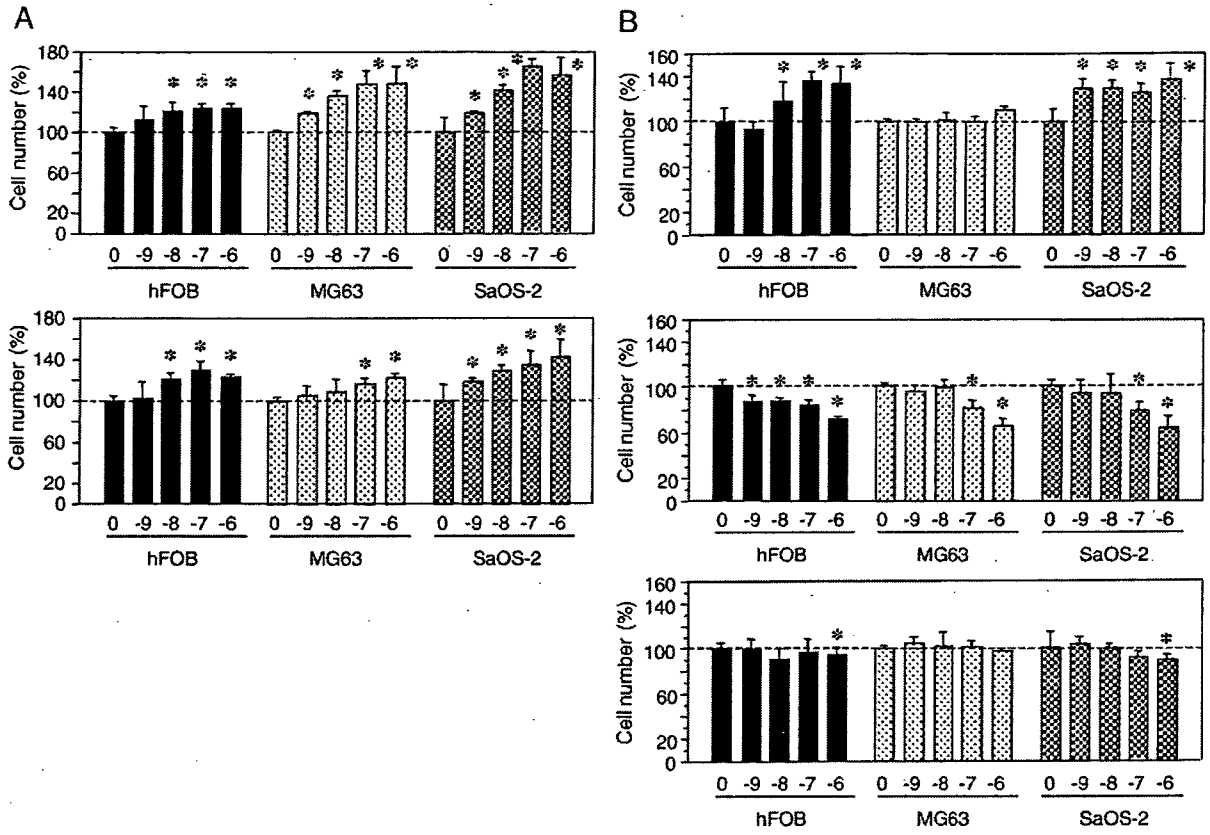

Fig. 3. (A) Proliferation of hFOB cells treated by estradiol (top) and 5α-DHT (bottom). *$p<0.05$ vs. vehicle control (0). (B) Proliferation of hFOB cells treated by exemestane (top), aminogluthetimide (middle), and Aromatase Inhibitor-I (bottom). *$p<0.05$ vs. vehicle control (0). $n=5$.

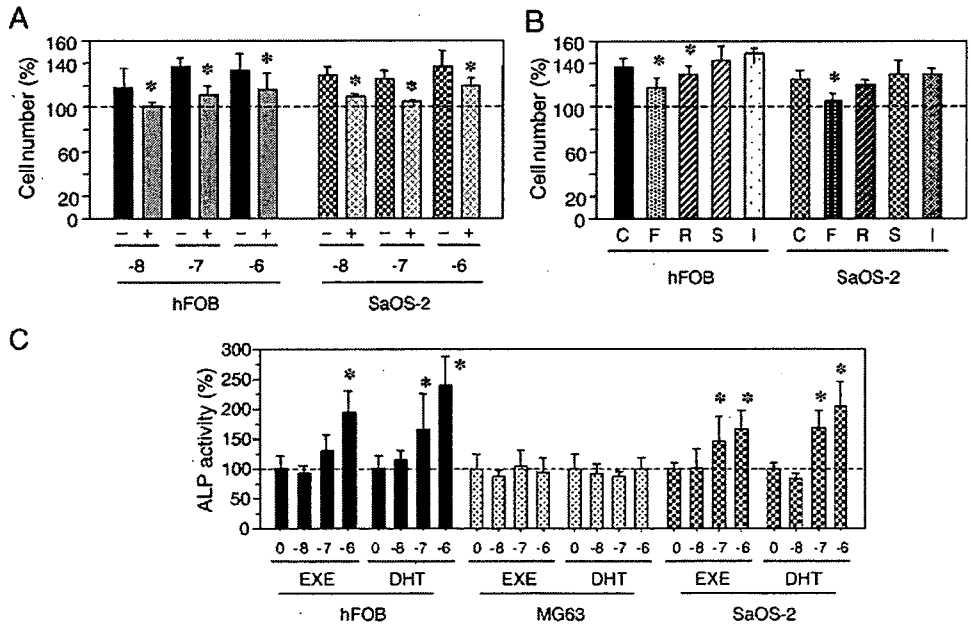

Fig. 4. (A) Effects of hydroxyflutamide on exemestane (10^{-8} to 10^{-6} M) stimulated the cell proliferation of both hFOB and Saos-2. With (+) or without (−) hydroxyflutamide, $p<0.05$ vs. without hydroxyflutamide (*). (B) Effects of steroid receptor blockers on exemestane (10^{-7} M) stimulated cell proliferation of hFOB and Saos-2. C, 10^{-7} M exemestane; F, hydroxyflutamide (5×10^{-6} M); R, RU38,486 (5×10^{-6} M); S, spironolactone (5×10^{-6} M); I, ICI182,720 (5×10^{-6} M). *$p<0.05$ vs. C (C) ALP activity in hFOB, Saos-2, MG-63 treated with exemestane (EXE, 10^{-8} to 10^{-6} M), or 5α-DHT (DHT, 10^{-8} to 10^{-6} M). *$p<0.05$ vs. vehicle control (0).

RT-PCR. Aromatase, ERα, ERβ, and AR were all detected in osteoblast-like cell lines, Saos-2 and MG-63 (Fig. 2B). In hFOB cell, expression of ERβ mRNA was more predominant than that of ERα mRNA. ERα mRNA as well as ERβ mRNA was detected in Saos-2 and MG-63 cells. The levels of AR mRNA expression in both hFOB and Saos-2 were significantly higher ($p=0.01$) than that in MG-63. ALP mRNA was also detected in intact hFOB, Saos-2, and MG-63 cells (data not present), respectively.

Estradiol and testosterone production

Results were summarized in Fig. 2C. The E2 levels in the medium of hFOB supplemented with Δ_4 treated with EXE or AI-I were significantly lower than that of cells without AIs. The levels of TST in the medium of hFOB supplemented with Δ4 treated with EXE or AI-I were significantly higher than that of cells without AIs.

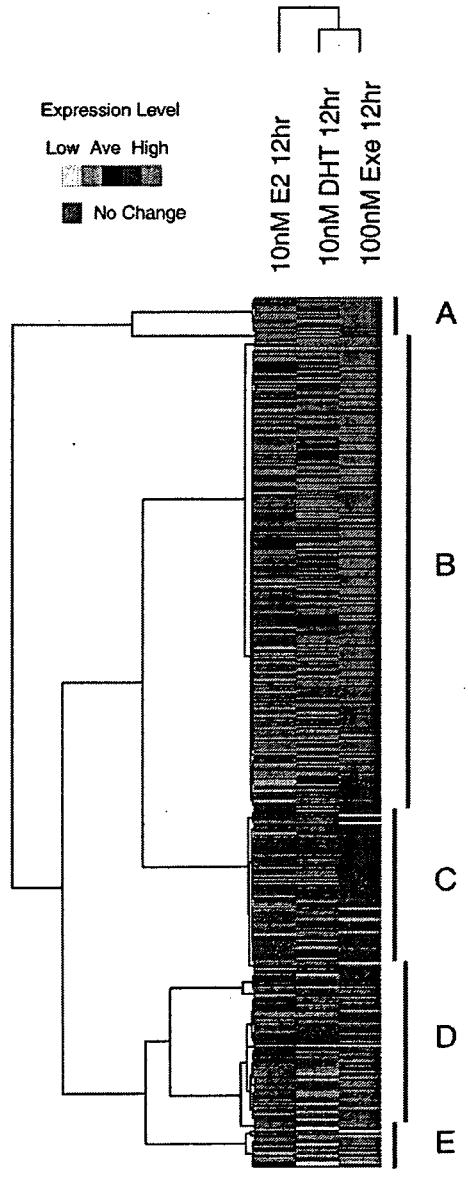

Fig. 5. In clustering analysis of the expression levels of each gene in hFOB cells treated with estradiol (E2), 5α-dihydrotestosterone (DHT), and exemestane (Exe).

Cell proliferation

Results of the cell proliferation assays are summarized in Figs. 3 and 4. There was a significant increment in the number of the cells after 72 h in hFOB, Saos-2, and MG-63 cells treated with 10^{-9} M (Saos-2 and MG-63) or 10^{-8} M (hFOB) to 10^{-6} M E2 (Fig. 3A). The cell number of hFOB and Saos-2 cells treated by 10^{-9} M (Saos-2) or 10^{-8} M (hFOB) to 10^{-6} DHT for 72 h was also significantly higher than control (Fig. 3A). The number of MG-63 cells was significantly increased only by high dose of DHT (10^{-7} M and 10^{-6} M) treatments (Fig. 3A). Prg (10^{-9} M to 10^{-6} M) treatments did not change the number of cells even after 72 h in all three cell lines examined (data not present).

Both EXE (Fig. 3B) and 17H-EXE (data not present) treatments of 10^{-8} M to 10^{-6} M, which were comparable to pharmacological inhibition doses of aromatization (Table 1), significantly increased the hFOB cell number for 72 h, respectively. In Saos-2 cells treated with relatively low dose, 10^{-9} to 10^{-6} M EXE, there was a significant increment in the number of the cells after 72 h (Fig. 3B). However, all the dose (10^{-9} M to 10^{-6} M) of EXE employed did not results in the change of cell number of MG-63 even after 72 h of treatment (Fig. 3B). The cell number of both hFOB and Saos-2 cells treated by both 10^{-6} M EXE and/or 17H-EXE for 48 h was also significantly higher than that treated for 24 h (data not present).

AGM treatment [10^{-9} (hFOB) or 10^{-7} (Saos-2 and MG-63) to 10^{-6} M] diminished the number of these three cells (Fig. 3B) and morphological changes in these cells were consistent with those caused by cytotoxic effects (data not present). AI-I treatment (10^{-9} to 10^{-7} M) was not associated with significant increment of the cell number in these cell lines (Fig. 3B). Only high dose (10^{-6} M) of AI-I significantly diminished the cell numbers of hFOB and Saos-2 but not of MG-63 (Fig. 3B).

The androgen receptor antagonist OHF (5×10^{-6} M) diminished the effects of EXE on these increments of both hFOB and Saos-2 cells (Figs. 4A and B). Treatment with RU but not spironolactone and ICI also inhibited EXE effects on hFOB cells (Fig. 4B).

ALP activity assay

Results of the ALP activity assay were summarized in Fig. 4C. There was a significant increment in the ALP activity of both hFOB and Saos-2 cells treated with 10^{-7} M (Saos-2) and/or 10^{-6} M (hFOB and Saos-2) EXE. Both 10^{-7} M and 10^{-6} M DHT treatment also increased the ALP activity in hFOB and Saos-2 cells, respectively. There were no changes of ALP activity in MG-63 treated with 10^{-8} M to 10^{-6} M of EXE and DHT, respectively.

Table 3a
Genes induced by exemestane treatment in hFOB cells—2.0 higher

	Gene title	Gene symbol	Raw data			Ratio	
			C	D	Ex	D	Ex
NM_002466	V-myb myeloblastosis viral oncogene homolog (avian)-like 2	**MYBL2**	70.9	156.9	150.3	2.2	2.1
AW444985	–	–	57.8	124.7	127.1	2.2	2.2
AF143684	Myosin IXB	MYO9B	48.3	64.4	122.2	1.3	2.5
NM_024682	TBC1 domain family, member 17	TBC1D17	31.7	37.6	64.8	1.2	2.0
BE965311	Chromosome 16 open reading frame 23	C16orf23	29.2	44.2	64.0	1.5	2.2
NM_004233	CD83 antigen (activated B lymphocytes, immunoglobulin superfamily)	CD83	29.0	66.5	60.9	2.3	2.1
AI806031	Skeletal muscle and kidney enriched inositol phosphatase	SKIP	27.7	48.6	55.4	1.8	2.0
AL136729	Ring finger protein 123	RNF123	20.0	23.7	41.3	1.2	2.1
NM_015254	Kinesin family member 13B	KIF13B	13.0	24.5	39.4	1.9	3.0
AL110249	Chromosome 20 open reading frame 194	C20orf194	13.4	39.0	29.7	2.9	2.2
AF208502	Early B-cell factor	EBF	12.5	21.1	28.5	1.7	2.3
AW007221	Solute carrier family 13 (sodium/sulfate symporters), member 4	SLC13A4	12.3	9.6	27.8	0.8	2.3
AB007458	TP53 activated protein 1	TP53AP1	12.6	22.2	26.2	1.8	2.1
AV713913	Osteopetrosis associated transmembrane protein 1	**OSTM1**	9.8	16.5	21.3	1.7	2.2
BF339201	THAP domain containing 6	THAP6	6.0	14.0	20.6	2.3	3.4
AK000455	Hypothetical gene MGC16733 similar to CG12113	MGC16733	7.3	16.6	18.8	2.3	2.6
AW974816	–	–	2.2	16.0	17.2	7.2	7.7
AK025325	Transcribed locus, moderately similar to NP_689573.2 zinc finger protein 573	–	7.3	11.4	16.2	1.6	2.2
NM_021192	Homeo box D11	**HOXD11**	5.3	16.2	15.8	3.0	3.0
NM_022169	ATP-binding cassette, sub-family G (WHITE), member 4	ABCG4	7.0	10.5	15.7	1.5	2.2
R62907	Disabled homolog 2, mitogen-responsive phosphoprotein (*Drosophila*)	DAB2	7.7	13.0	15.5	1.7	2.0
NM_002661	Phospholipase C, gamma 2 (phosphatidylinositol-specific)	PLCG2	7.3	12.3	15.3	1.7	2.1
BG393032	Solute carrier family 13 (sodium/sulfate symporters), member 4	SLC13A4	6.4	6.7	15.1	1.0	2.3
BC002794	Tumor necrosis factor receptor superfamily, member 14	TNFRSF14	6.2	11.3	13.6	1.8	2.2
BC042908	KIAA0690	KIAA0690	5.6	7.4	13.5	1.3	2.4
AW451961	Adenylate cyclase activating polypeptide 1 (pituitary) receptor type I	**ADCYAP1R1**	4.3	11.7	13.2	2.7	3.1
AI863264	Glypican 2 (cerebroglycan)	**GPC2**	5.3	7.2	13.2	1.3	2.5
AF130050	ACA47 scaRNA gene	-	5.6	9.5	12.9	1.7	2.3
AK022326	Hypothetical gene supported by AK022326	-	6.1	12.7	12.9	2.1	2.1
AK021807	Low density lipoprotein receptor-related protein 11	LRP11	5.9	6.2	12.8	1.0	2.2
AU155415	Kallikrein 7 (chymotryptic, stratum corneum)	KLK7	5.6	13.5	12.7	2.4	2.3
BF673779	Hypothetical protein FLJ30834	FLJ30834	5.5	6.3	12.3	1.1	2.2
AV646335	–	–	2.6	13.0	11.2	5.0	4.3
BC040600	–	–	5.0	5.4	10.6	1.1	2.1
AI131035	–	–	5.1	9.2	10.5	1.8	2.1

C, vehicle control; D, 5α-dihydrotestosterone; Ex, exemestane. Genes that performed quantitative RT-PCR were described in bold style.

Microarray/clustering analysis

In hFOB cells, the hierarchical clustering analysis contains 430 genes which demonstrated expression ratios above 2.0-fold and below 0.5-fold compared with vehicle control cells after 12 h of each gene treated with 10^{-8} M E2, 10^{-8} M DHT, or 10^{-7} M EXE. The expression profiles of EXE treated cells were closely related to those of DHT (Fig. 5). In this study, we focused on 35 genes (Table 3a), which were all up-regulated twice or more than control. In this group, we further focused on 5 genes, B-Myb 2 (MYBL2), osteopetrosis associated transmembrane protein 1 (OSTM1), homeo box D 11 (HOXD11), adenylate cyclase activating polypeptide 1 receptor (ADCYAP1R1), and glypican 2 (GPC2) which are all considered to play important roles in EXE or DHT induced cell proliferation. We therefore examined whether these 5 genes were increased by EXE or DHT treatments using quantitative RT-PCR in hFOB cells. We also examined the validation of results of microarray analysis obtained in hFOB cells in Saos-2 and MG-63 cells.

Validation of microarray analysis using quantitative RT-PCR

In hFOB cells, all of these 5 genes described above were significantly increased by 10^{-7} M EXE treatment, and 3/5 genes (except for OSTM1 and GPC2) were also significantly increased by 10^{-8} M DHT treatment. HOXD11 and ADCYAP1R1 genes increased by both EXE and DHT were significantly diminished by OHF (5×10^{-6} M) treatment (Figs. 6A–C).

The similar results of changes of MYBL2 expression were also obtained in both Saos-2 and MG-63 treated with EXE and DHT, respectively (Fig. 6A). In addition, the results of HOXD11 expression in hFOB were equivalent to those in Saos-2 but not in MG-63 treated with EXE and DHT (Fig. 6B). Other genes induced by treatment of EXE and DHT in hFOB such as OSTM1, GPC2, and ADCYAP1R1 were not changed in both Saos-2 and MG-63 cells treated with EXE and DHT, respectively (data not present). AI-1 or AGM treatment did not increase all of these genes expression in hFOB (data not present).

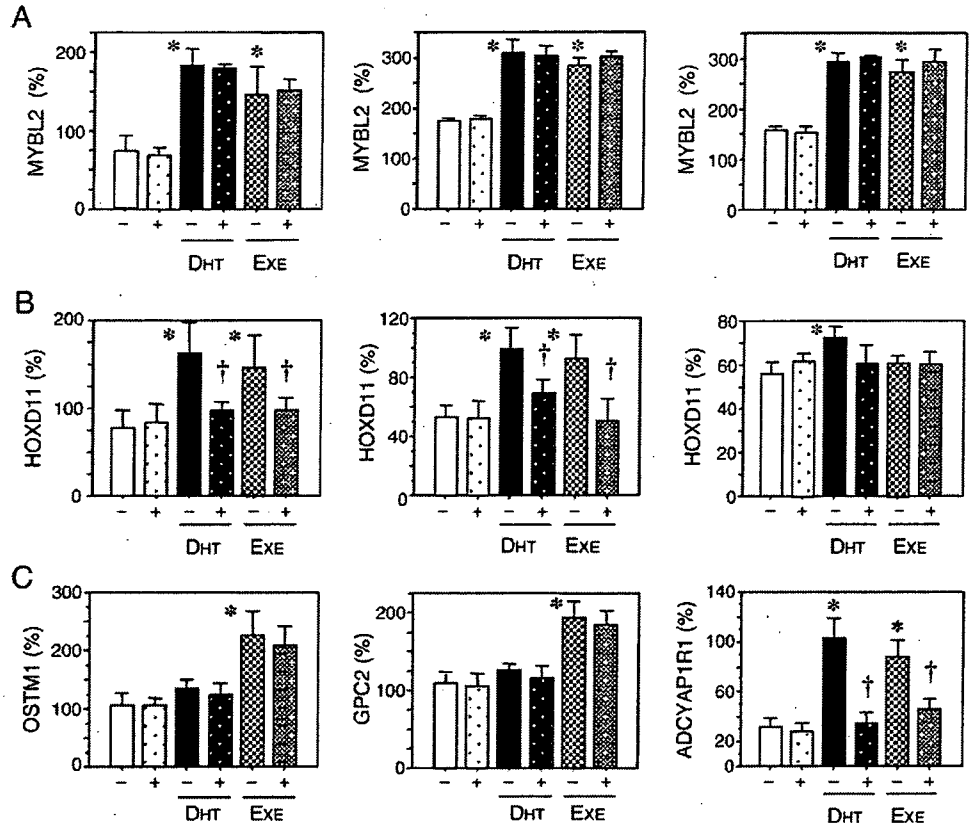

Fig. 6. Validation of microarray analysis. (A) Expression levels of MYBL2 in hFOB (left), Saos-2 (middle), and MG-63 (right). (B) Expression levels of HOXD11 in hFOB (left), Saos-2 (middle), and MG-63 (right). (C) Expression levels of OSTM1, GPC2, and ADCYAP1R1 in hFOB. DHT: 10^{-8} M 5α-dihydrotestosterone, EXE: 10^{-7} M Exemestane, with (+) or without (−) hydroxyflutamide, $p<0.05$ vs. control (*) or without hydroxyflutamide (†).

Analysis of osteoblast growth-related genes

Results of microarray analysis in hFOB cell demonstrated that osteoblast growth-related genes [24,25] such as COL1A1, SMAD1, SMAD5, SPARC, and RUNX2 were all up-regulated by exemestane (10^{-7} M) treatment but the degrees of increment were all under 2-fold (Table 3b). In this microarray analysis, other expression levels of previously reported osteoblast-related genes were not altered.

In hFOB cells, the validation analysis of these genes described above using quantitative RT-PCR (Fig. 7) demonstrated that 4/5 genes (except for COL1A1) were significantly increased by 10^{-7} M EXE treatment, and 4/5 genes (except for SMAD1) were also significantly increased by 10^{-8} M DHT treatment. The increased expression of the SMAD1, SMAD5, and SPARC genes by EXE or DHT, was significantly diminished by OHF (5×10^{-6} M) treatment. There were no effects of OHF pretreatment on the increased expression levels of RUNX2 that had occurred after both EXE and DHT treatments. Both AI-I and AGM treatment could not increase all of these genes expression in hFOB (data not present).

In Saos-2 cells, 4/5 genes (except for RUNX2) were significantly increased by 10^{-7} M EXE treatment, and 3/5 genes (except for RUNX2 and SMAD1) were also significantly increased by 10^{-8} M DHT treatment. The increment of the COL1A1, SMAD5, and SPARC genes expression by EXE or DHT, was significantly diminished by OHF (5×10^{-6} M) treatment. All of these 5 genes did not change in MG-63 cells treated with EXE or DHT, respectively (data not present).

Immunohistochemistry of AR

Marked AR immunoreactivity was detected in the nuclei of osteoblasts or lining cells but not in osteoclasts in four cases (Fig. 8). In these four cases, AR immunoreactivity was also detected in osteocytes and condrocytes. In one case, there was no immunoreactivity in all types of bone cells.

Discussion

In the clinical study of EXE compared to placebo administrated for two years [26,27], EXE modestly enhanced bone loss from the femoral neck without significant influence on lumber bone loss despite a marked systemic estrogen depletion. Furthermore, the risks of clinical bone fractures are considered to be lower with EXE treatment than that seen with non steroidal AIs [27,28], though it is also important to recognize that EXE has not been shown to significantly increase the amount of bone mass in various clinical studies of breast cancer patients [26,27]. The relative protective effect of EXE, a

Table 3b
Genes induced by exemestane treatment in hFOB cells—the osteoblast growth-related genes

	Gene title	Gene symbol	Raw data			Ratio	
			C	D	Ex	D	Ex
K01228	Collagen, type I, alpha 1	**COL1A1**	2797.2	3240.9	3058.5	1.2	1.1
BE221212	Collagen, type I, alpha 1	**COL1A1**	2741.1	3048.3	3052.2	1.1	1.1
AI743621	Collagen, type I, alpha 1	**COL1A1**	228.0	241.6	242.5	1.1	1.1
AA788711	Collagen, type I, alpha 2	COL1A2	2250.6	2474.3	2375.4	1.1	1.1
NM_000089	Collagen, type I, alpha 2	COL1A2	1749.1	1848.7	1787.6	1.1	1.0
M60485	Fibroblast growth factor receptor 1	FGFR1	178.9	185.7	198.6	1.0	1.1
BE467261	Fibroblast growth factor receptor 1	FGFR1	165.4	208.6	189.7	1.3	1.1
M63889	Fibroblast growth factor receptor 1	FGFR1	119.3	111.6	140.5	0.9	1.2
NM_023110	Fibroblast growth factor receptor 1	FGFR1	60.5	84.0	70.2	1.4	1.2
AU145411	Fibroblast growth factor receptor 1	FGFR1	29.2	44.1	37.5	1.5	1.3
AI359368	Fibroblast growth factor receptor 3	FGFR3	41.4	65.5	58.7	1.6	1.4
NM_001552	Insulin-like growth factor binding protein 4	IGFBP4	809.1	1027.5	1040.4	1.3	1.3
AL353944	Runt-related transcription factor 2	**RUNX2**	192.9	226.3	216.3	1.2	1.1
AU146891	SMAD, mothers against DPP homolog 1 (*Drosophila*)	**SMAD1**	161.2	195.6	204.6	1.2	1.3
NM_005901	SMAD, mothers against DPP homolog 2 (*Drosophila*)	SMAD2	100.3	108.2	113.7	1.1	1.1
NM_005902	SMAD, mothers against DPP homolog 3 (*Drosophila*)	SMAD3	110.2	106.5	127.7	1.0	1.2
BF526175	SMAD, mothers against DPP homolog 5 (*Drosophila*)	**SMAD5**	361.0	488.3	514.2	1.4	1.4
AI478523	SMAD, mothers against DPP homolog 5 (*Drosophila*)	SMAD5	300.7	384.9	346.9	1.3	1.2
AF010601	SMAD, mothers against DPP homolog 5 (*Drosophila*)	SMAD5	79.2	99.7	87.6	1.3	1.1
AY014180	SMAD-specific E3 ubiquitin protein ligase 2	SMURF2	804.2	844.7	851.8	1.1	1.1
AU157259	SMAD-specific E3 ubiquitin protein ligase 2	SMURF2	77.1	81.5	86.3	1.1	1.1
AL575922	Secreted protein, acidic, cysteine-rich (osteonectin)	**SPARC**	1702.1	1935.5	1925.8	1.1	1.1
BF508662	Sprouty homolog 1, antagonist of FGF signaling (*Drosophila*)	SPRY1	31.9	46.3	45.4	1.5	1.4
NM_014886	TGF beta-inducible nuclear protein 1	TINP1	1185.7	1259.5	1241.1	1.1	1.0

C, vehicle control; D, 5α-dihydrotestosterone; Ex, exemestane. Genes that performed quantitative RT-PCR were described in bold style.

steroidal aromatase inhibitor, has been therefore attributed to its actions through AR in osteoblasts. Systemic androgenic effects such as hypertricosis, hair loss, hoarseness, and acne have been reported only in 4% [6] of the patients treated with EXE (25 mg/day) and the frequency of these effects increases to approximately 10% in those treated with higher dose 200 mg/day of EXE [6]. This finding suggests that the patients treated with EXE are under relatively weak systemic androgenic effects. Androgen sensitivity has been well-known to be subject to great individual variation caused by AR gene CAG polymorphism in women as well as men [29,30]. Therefore, this 5 to 10% of the patients who manifested clinical androgenic effects by EXE treatment may be individuals associated with relatively enhanced androgenic sensitivity. Replacement therapy with TST is generally effective at restoring bone in hypogonadal men [31]. In female-to-male, genetic female transsexual subjects, high-dose TST therapy generally increased BMD at the femoral neck, despite decrement of E2 to postmenopausal levels [32,33]. Therefore, androgens may play an important role in bone protection in women as well as men.

The results of cell proliferation assay demonstrated that the cell number of MG-63 was increased by both E2 and DHT treatments, but the dose of DHT was relatively higher than that in two other cells. MG-63 expressed higher levels of ERα/β mRNA, but the level of AR mRNA was lower than that in both Saos-2 and hFOB. Both cell proliferation and ALP activity of MG-63 could not be stimulated by EXE treatment. Molecular mechanisms of androgen actions on osteoblasts have remained largely unknown. Androgen is well-known to stimulate osteoblast proliferation [34] and differentiation [35]. For instance, osteoprotegerin mRNA was increased by TST as well as DHT treatments in mouse 3T3-E1 cells [36].

AR and ERβ but not ERα are predominantly detected in osteoblasts located on human cancellous bone using immunohistochemical analysis [37]. Therefore, hFOB examined in this study is considered to maintain relatively native status of sex steroids pathways in human osteoblasts. Therefore, we employed hFOB for further examination of EXE effects on osteoblast gene expression pattern using microarray analysis. In this study, we demonstrated that the genes MYBL2 [38], OSTM1 [39], HOXD11 [40], ADCYAP1R1 [41], and GPC2 [42] were target genes of EXE alone or both EXE and DHT in hFOB using microarray/PCR analysis. These genes were demonstrated to be involved in regulation of cell cycle, differentiation, and transcription. In EXE or DHT treatment in hFOB and Saos-2, in which cells proliferations were stimulated, an increased expression of HOXD11 gene was detected. The product of the mouse Hoxd11 gene was reported to play a role in forelimb morphogenesis [40,43]. Therefore, these finding suggest that osteoblast cell proliferation stimulated by EXE treatment may depend on HOXD11 gene expression through AR. In this study, the cell proliferation of MG-63, which expressed relatively low level of AR, was not stimulated by EXE. In addition, HOXD11 gene expression was not up-regulated by EXE treatment in MG-63 cells. These results were also consist with the protective effects of EXE through potential androgen-HOXD11 pathway in osteoblast cells. In this study, we also examined the effects of EXE and DHT on osteoblast growth-related genes using micro-

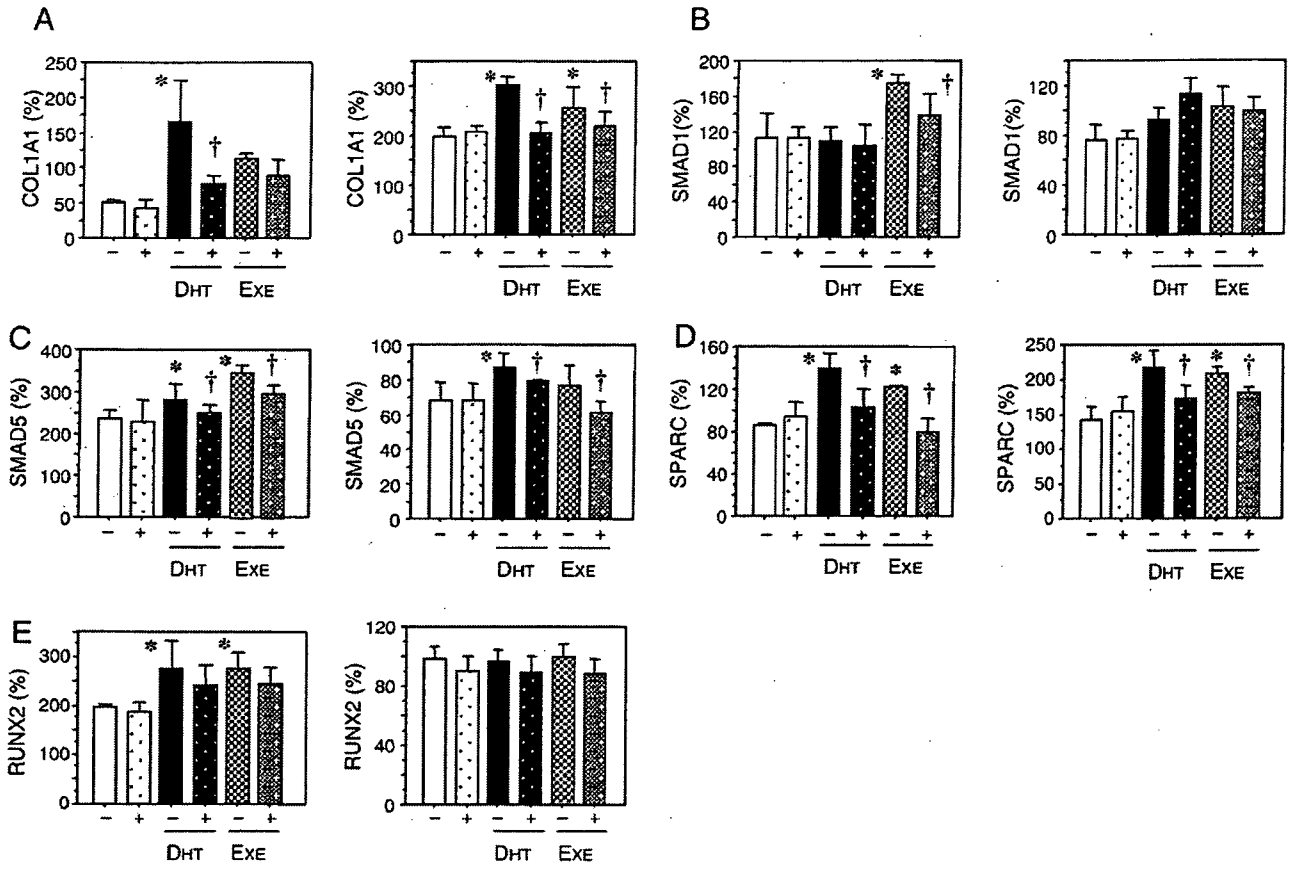

Fig. 7. Expression levels of osteoblast growth-related genes in hFOB (left) and Saos-2 (right). DHT: 10^{-8} M 5α-dihydrotestosterone, EXE: 10^{-7} M Exemestane, with (+) or without (−) hydroxyflutamide, $p<0.05$ vs. control (*) or without hydroxyflutamide (†).

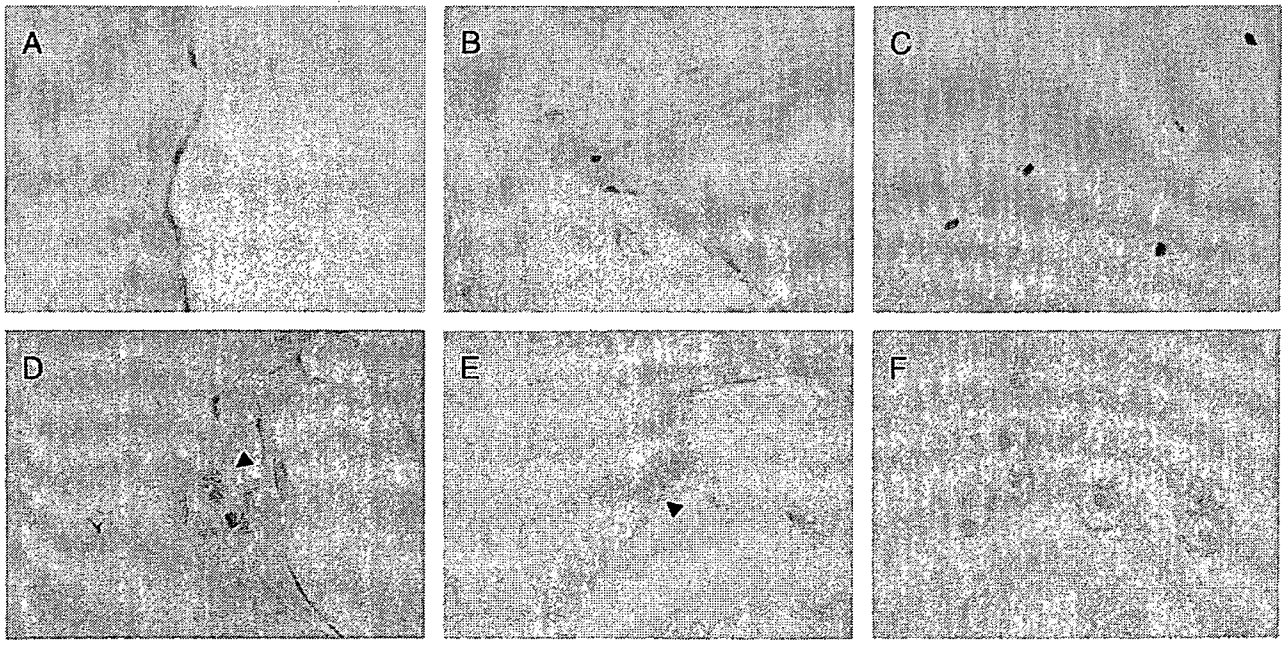

Fig. 8. Immunohistochemistry of androgen receptor in human bone tissues. Immunoreactivity of androgen receptor was detected in nuclei of osteoblasts/liner cells (A, B) but not in osteoclasts (D, E; arrowheads). Immunoreactivity of androgen receptor was also detected in nuclei of osteocytes (C) and condrocytes (F).

array analysis and following quantitative RT-PCR. COL1A1, SMAD5, and SPARC (osteonectine) were up-regulated by EXE and/or DHT treatments in both hFOB and Saos-2 cells. EXE or DHT treatments in both hFOB and Saos-2 also resulted in increased ALP activity. There have been, however, no studies reported on whether these genes are primary or secondary androgen responsive genes in osteoblasts. The AR-specific antagonist, OHF demonstrated no inhibitory effects on RUNX2 expression increased by EXE or DHT treatment in hFOB cells. In addition, hFOB cell growth induced by high dose of EXE treatment was not completely inhibited by OHF treatment. These results all suggest that EXE also may stimulate hFOB cell proliferation through both AR dependent and independent pathways. From our data of steroid production in hFOB, EXE may have an additional androgenic effect through increased TST levels in conjunction with inhibition of aromatization in hFOB cells. However, it awaits further investigations for clarification.

In normal bone remodeling, bone formation by osteoblasts follows bone resorption by osteoclasts and occurs in a precise and quantitative manner (coupling). In this coupling between bone formation and resorption, a coupling factor that induces bone formation is considered to be released during osteoclastic bone resorption [44]. This study has focused on the specific effects on osteoblast cells. However, it is true that there were significant increases in both serum bone formation and resorption markers in postmenopausal women administered with EXE for 2 years [26]. Osteoclasts, which are responsible for bone resorption, are target cells for many anti-osteoporosis therapeutic agents such as bisphosphonate of postmenopausal women [45]. However, it is unclear whether EXE acts on osteoclast directly. Chen et al. [46] reported that testosterone inhibited osteoclast formation stimulated by parathyroid hormone through the AR but not through the production of intrinsic estrogen using primary mouse osteoclast cells. In both human and rodent bone tissues, AR is expressed in both osteoblasts and osteocytes [47,48]. However, AR is detected in osteoclasts of rodent but not in human cells [31,47,48]. Therefore, in humans, androgens are considered to exert their effects on bone through osteoblasts. EXE may therefore exert its possible androgenic effects on human bone through osteoblasts but not osteoclasts. Results of our present study also suggest the possible roles of EXE on osteoblast cells through AR independent manner. Results of clinical studies suggest that the combination therapy of AI and COX-2 inhibitors could provide more effective aromatase inhibition than single therapy in hormone-sensitive postmenopausal breast cancer [49]. Bone resorption induced by IL-1 and IL-6 was also reported to occur via stimulation of COX-2 dependent PGE_2 production in osteoblasts *in vitro* [50]. Therefore, further investigations are required to clarify the effects of AI including EXE on human bone tissues.

In summary, this study using osteoblast and osteoblast-like cell lines suggested the potential protective effect of steroidal AI, EXE on osteoblasts occurred through both AR dependent and independent pathways. HOXD11 gene known as bone morphogenesis factor and osteoblast growth-related genes were induced by EXE treatment as well as DHT treatment in both hFOB and Saos-2. Damages of bone tissues by estrogen depletion caused by AI administration are considered unavoidable but the selection of potential hormone therapies which could minimize the damages or injuries of bone tissues is considered important.

Acknowledgments

We appreciate Dr. Shin-ichi Hayashi (Divisions of Molecular Medical Technology, Tohoku University School of Medicine) for critical comments. We also appreciate Ms. Chika Tazawa, Ms. Toshie Suzuki, Ms. Miki Mori and Mr. Katsuhiko Ono (Department of Pathology, Tohoku University School of Medicine) for skillful technical assistances. This research was supported by Grant-in-aid for Health and Labor Sciences Research Grant on Risk of Chemical Substances (H16-Kagaku-002) from Ministry of Health, Labor, and Welfare, Japan and Kanzawa Medical Research Foundation, Nagano, Japan.

References

[1] Rogers J. Estrogens in the menopause and postmenopause. N Engl J Med 1969;280:364–7.
[2] Wingate L. The epidemiology of osteoporosis. J Med 1984;15:245–66.
[3] Felson DT, Zhang Y, Hannan MT, Kiel DP, Wilson PW, Anderson JJ. The effect of postmenopausal estrogen therapy on bone density in elderly women. N Engl J Med 1993;329:1141–6.
[4] Lester L, Coleman R. Bone loss and the aromatase inhibitors. Br J Cancer 2005;93:S16–22.
[5] Miller WR, Dixon JM. Antiaromatase agents: preclinical data and neoadjuvant therapy. Clin Breast Cancer 2000;1:S9–S14.
[6] Lønning PE, Paridaens R, Thurlimann B, Piscitelli G, di Salle E. Exemestane experience in breast cancer treatment. J Steroid Biochem Mol Biol 1997;61:151–5.
[7] Center for Drug Evaluation and Research Application Number NDA 20753 (Exemestane) Medical Review. Food and Drug Administration, 1999.
[8] Goss PE, Qi S, Josse RG, Pritzker KPH, Mendes M, Hu H, et al. The steroidal Aromatase inhibitor exemestane prevent bone loss in ovariectomized rats. Bone 2004;34:384–92.
[9] Goss PE, Qi S, Cheung AM, Hu H, Mendes M, Pritzker KPH. Effects of steroidal aromatase inhibitor exemestane and the nonsteroidal aromatase inhibitor letrozole on bone and lipid metabolism in the ovariectomized rats. Clin Cancer Res 2004;10:5717–23.
[10] Sasano H, Uzuki M, Sawai T, Nagura H, Matsunaga G, Kashimoto O, et al. Aromatase in human bone tissue. J Bone Miner Res 1997;12:1416–23.
[11] Schweikert HU, Wolf L, Romalo G. Oestrogen formation from Androstendione in human bone. Clin Endocrinol 1995;43:37–42.
[12] Purohit A, Flanagan AM, Reed MJ. Estrogen synthesis by osteoblast cell lines. Endocrinology 1992;131:2027–9.
[13] Tanaka S, Haji M, Nishi Y, Yanase T, Takayanagi R, Nawata H. Aromatase activity in human osteoblast-like osteosarcoma cell. Calcif Tissue Int 1993;52:107–9.
[14] Recanatini M, Bisi A, Cavalli A, Belluti F, Gobbi S, Rampa A, et al. A new class of nonsteroidal aromatase inhibitors: design and synthesis of chromone and xanthone derivatives and inhibition of the P450 enzymes aromatase and 17 alpha-hydroxylase/C17,20-lyase. J Med Chem 2001;44:672–80.
[15] Linkhart TA, Mohan S, Baylink DJ. Growth factors for bone growth and repair: IGF, TGF beta and BMP. Bone 1996;19:1S–12S.
[16] Harris SA, Enger RJ, Riggs BL, Spelsberg TC. Development and characterization of a conditionally immortalized human fetal osteoblastic cell line. J Bone Miner Res 1995;10:178–86.
[17] Suzuki T, Darnel AD, Akahira JI, Ariga N, Ogawa S, Kaneko C, et al. 5alpha-reductases in human breast carcinoma: possible modulator of in situ androgenic actions. J Clin Endocrinol Metab 2001;86:2250–7.

[18] Miki Y, Suzuki T, Tazawa C, Ishizuka M, Semba S, Gorai I, et al. Analysis of gene expression induced by diethylstilbestrol (DES) in human primitive Müllerian duct cells using microarray. Cancer Lett 2005;220:197–210.
[19] Yamamoto M, Takahashi Y, Tabata Y. Controlled release by biodegradable hydrogels enhances the ectopic bone formation of bone morphogenetic protein. Biomaterials 2003;24:4375–83.
[20] Kanno J, Aisaki K, Igarashi K, Nakatsu N, Ono A, Kodama Y, et al. "Per cell" normalization method for mRNA measurement by quantitative PCR and microarrays. BMC Genomics 2006;29:64.
[21] Eisen MB, Spellman PT, Brown PO, Bostein D. Cluster analysis and display of genome-wide expression patterns. Proc Natl Acad Sci U S A 1998;95:14863–8.
[22] Miki Y, Nakata T, Suzuki T, Darnel AD, Moriya T, Kaneko C, et al. Systemic distribution of steroid sulfatase and estrogen sulfotransferase in human adult and fetal tissues. J Clin Endcrinol Metab 2002;87:5760–8.
[23] Ishizuka M, Hatori M, Suzuki T, Miki Y, Darnel AD, Tazawa C, et al. Sex steroid receptors in rheumatoid arthritis. Clin Sci (Lond) 2004;106: 293–300.
[24] Rodan GA, Noda M. Gene expression in osteoblastic cells. Crit Rev Eukaryot Gene Expr 1991;1:85–98.
[25] Ito Y, Miyazono K. RUNX transcription factors as key role of TGF-β superfamily signaling. Curr Opin Genet Dev 2003;13:43–7.
[26] Lønning PE, Geisler J, Krag LE, Erikstein B, Bremnes Y, Hagen AI, et al. Effects of exemestane administered for 2 years versus placebo on bone mineral density, bone biomarkers, and plasma lipids in patients with surgically respected early breast cancer. J Clin Oncol 2005;23:4847–9.
[27] Coombes RC, Hall E, Gibson LJ, Paridaens R, Jassem J, Delozier T, et al. Intergroup Exemestane Study. A randomized trial of exemestane after two to three years of tamoxifen therapy in postmenopausal women with primary breast cancer. N Engl J Med 2004;350:1081–92.
[28] Coleman RE, Banks LM, Girgis SI, Vrdoljak E, Fox J, Porter LS, et al. Skeletal effect of exemestane in the Intergroup Exemestane Study (IES)—2 years bone mineral density (BMD) and bone biomarker data. Breast Cancer Res Treat 2005;94:S233.
[29] Vottero A, Stratalis CA, Ghizzoni L, Longui CA, Karl M, Chrousos GP. Androgen receptor-mediated hypersensitivity to androgen in women with nonhyperandrogenic hirsutism: skewing of X-chromosome inactivation. J Clin Endocrinol Metab 1999;84:1091–5.
[30] Brum IS, Spritzer PM, Paris F, Maturana MA, Audran F, Sultan C. Association between androgen receptor gene CAG repeat polymorphism and plasma testosterone levels in postmenopausal women. J Soc Gynecol Investig 2005;12:135–41.
[31] Vanderschueren D, Vandenput L, Boonen S, Lindberg MK, Bouillon R, Ohlsson C. Androgens and bone. Endocr Rev 2004;25:389–425.
[32] Turner A, Chen T, Barber T, Malabanan A, Holick M, Tangpricha V. Testosterone increases bone mineral density in female-to-male transsexuals: a case series of 15 subjects. Clin Endocrinol (Oxf) 2004;61:560–6.
[33] Ruetsche AG, Kneubuehl R, Birkhaeuser MH, Lippuner K. Cortical and trabecular bone mineral density in transsexuals after long-term cross-sex hormonal treatment: a cross-sectional study. Osteoporos Int 2005;16: 791–98.
[34] Kasperk CH, Wergedal JE, Farley JR, Linkhart TA, Turner RT, Baylink DJ. Androgens directly stimulate proliferation of bone cells in vitro. Endocrinology 1989;124:1576–8.
[35] Kasperk C, Fitzsimmons R, Strong D, Mohan S, Jennings J, Wergedal J, et al. Studies of the mechanism by which androgens enhance mitogenesis and differentiation in bone cells. J Clin Endocrinol Metab 1990;71:1322–9.
[36] Chen Q, Kaji H, Kanatani M, Sugimoto T, Chihara K. Testosterone increases osteoprotegerin mRNA expression in mouse osteoblast cells. Horm Metab Res 2004;36:674–8.
[37] Bord S, Horner A, Beavan S, Compston J. Estrogen receptors alpha and beta are differentially expressed in developing human bone. J Clin Endocrinol Metab 2001;86:2309–14.
[38] Sala A, Watson R. B-Myb protein in cellular proliferation, transcription control, and cancer: latest developments. J Cell Physiol 1999;179:245–50.
[39] Chalhoub N, Benachenhou N, Rajapurohitam V, Pata M, Ferron M, Frattini A, et al. Grey-lethal mutation induces severe malignant autosomal recessive osteopetrosis in mouse and human. Nat Med 2003;9:399–406.
[40] Boulet AM, Capecchi MR. Multiple roles of Hoxa11 and Hoxd11 in the formation of the mammalian forelimb zeugopod. Development 2004; 131:299–309.
[41] Lundberg P, Lundgren I, Mukohyama H, Lehenkari PP, Horton MA, Lerner UH. Vasoactive intestinal peptide (VIP)/pituitary adenylate cyclase-activating peptide receptor subtypes in mouse calvarial osteoblasts: presence of VIP-2 receptors and differentiation-induced expression of VIP-1 receptors. Endocrinology 2001;142:339–47.
[42] Gutierrez J, Osses N, Brandan E. Changes in secreted and cell associated proteoglycan synthesis during conversion of myoblasts to osteoblasts in response to bone morphogenetic protein-2: role of decorin in cell response to BMP-2. J Cell Physiol 2006;206:58–67.
[43] Omi M, Fisher M, Maihle NJ, Dealy CN. Studies on epidermal growth factor receptor signaling in vertebrate limb patterning. Dev Dyn 2005;233:288–300.
[44] Rodan GA, Raisz LG, Bilezikian JP. Pathophysiology of osteoporosis. . (chapter 73)In: Bilezikian JP, Raisz LG, Rodan GA, editors. Principles of bone biology, 2nd ed., vol. 1. NY, USA: Academic Press, A division of Harcourt, Inc.; 2002. p. 1275–90.
[45] Kellinsalmi M, Monkkonen H, Monkkonen J, Leskela HV, Parikka V, Hamalainen M, et al. In vitro comparison of clodronate, pamidronate and zoledronic acid effects on rat osteoclasts and human stem cell-derived osteoblasts. Basic Clin Pharmacol Toxicol 2005;97:382–91.
[46] Chen Q, Kaji H, Sugimoto T, Chihara K. Testosterone inhibits osteoclast formation stimulated by parathyroid hormone through androgen receptor. FEBS Lett 2001;491:91–3.
[47] Abu EO, Horner A, Kusec V, Triffitt JT, Compston JE. The localization of androgen receptors in human bone. J Clin Endocrinol Metab 1997; 82:3493–7.
[48] Wiren KM, Orwoll ES. Androgens: receptor expression and steroid action in bone. . (chapter 43)In: Bilezikian JP, Raisz LG, Rodan GA, editors. Principles of bone biology, 2nd ed., vol. 1. NY, USA: Academic Press, A division of Harcourt, Inc.; 2002. p. 757–72.
[49] Chow LW, Wong JL, Toi M. Celecoxib anti-aromatase neoadjuvant (CAAN) trial for locally advanced breast cancer: preliminary report. J Steroid Biochem Mol Biol 2003;86:443–7.
[50] Sato T, Morita I, Sakaguchi K, Nakahama KI, Smith WL, Dewitt DL, et al. Involvement of prostaglandin endoperoxide H synthase-2 in osteoclast-like cell formation induced by interleukin-1 beta. J Bone Miner Res 1996;11:392–400.

関節リウマチにおける軟骨・骨破壊の病理学的特徴

宇月 美和[*1)] 佐々木 喜子[**] 澤井 高志[*2)]

最近は遺伝子や細胞内タンパクなどを問題にした解析が目覚ましい発展を遂げ，ともすれば全体像をみることが失われがちである。本稿では，関節リウマチ（RA）の組織学的所見を中心にして滑膜の炎症から軟骨・骨破壊に至る過程を述べた。RAの病態を炎症という一つの流れに従って眺めてみると，まだまだ解明されるべき点が多いことに気がつく。たまには立ち止まって全体像を眺めることも必要ではないかと思われる。

Histopathological Features of Joint Destruction in Rheumatoid Arthritis (RA).

Iwate Medical University, School of Medicine, Department of Pathology
Miwa Uzuki, Takashi Sawai

Iwate Medical University, School of Medicine, Department of Pathology/Orthopedics
Yoshiko Sasaki

Recent technologies proceed the remarkable development of genetical and protein analysis. However, we are apt to lose opportunities to observe about the disease as a whole feature. In this article, we describe the inflammatory process from synovial inflammation to cartilage and bone destruction. We notice that there are many problems to be solved in rheumatoid arthritis (RA) from the point of inflammatory process. It is often needed for us to stand still and look over the whole features of disease.

はじめに

関節リウマチ（RA）は免疫異常を基盤とした慢性炎症性疾患であるが，その大きな特徴は滑膜の炎症と軟骨・骨の吸収であり，疼痛を伴った関節は最終的には変形と運動障害に至る（図1，2）。疾患の本体はまだ十分に解明されたとは言い難いが，滑膜組織の炎症の特徴については比較的よく観察されており，そこに発現しているさまざまな炎症性細胞，サイトカインや増殖因子，タンパク分解酵素などの解析が行われている[1~7]。

*岩手医科大学病理学第一講座 *1)（うづき・みわ） *2)教授（さわい・たかし）
**岩手医科大学病理学第一講座/整形外科学講座（ささき・よしこ）

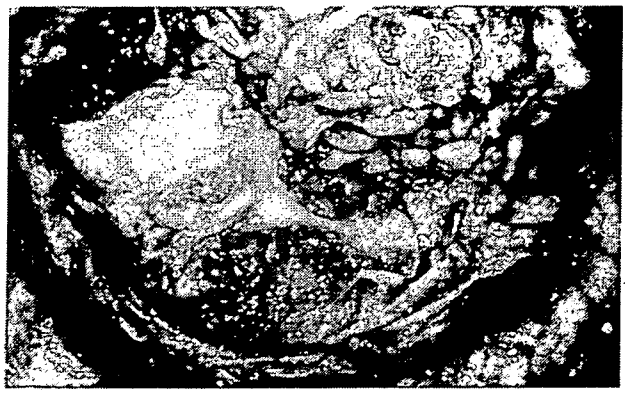

図1　RA患者の膝関節の手術所見

血管の豊富な炎症性肉芽組織（パンヌス）によって滑らかな関節の表面は侵食されていく。
RA：関節リウマチ

（筆者ら提供）

図2　パンヌスの組織所見

パンヌスは腫瘍の浸潤のように軟骨を吸収し，下方にある骨へ至り，これを吸収する。

（筆者ら提供）

一方，骨破壊は，一般的には滑膜の炎症がそのまま骨組織に波及して軟骨や骨を破壊するか，あるいは破骨細胞を活性化して骨を壊すとイメージされていると思われるが，実際はそう単純ではない。例えば，軟骨組織は血管が侵入すると変性するが，骨は循環障害によって骨変性が起こるなど，対照的な反応を示す。

では，RAの関節破壊とはどのような形で進行するのであろうか。これを明らかにするためには，破骨細胞の動態，サイトカインの発現，タンパク分解酵素の個別的な活性とは別に，細胞や組織がどのような形で変化していくかという過程について，組織を通して全体的な面から眺めることも必要と思われる。

RAの炎症はどこから始まるか

関節の炎症の始まりはどこかということに関しては諸説がある。RA初期の病理組織像については，①浮腫，②細胞浸潤，③フィブリンの析出と言われているが，どこから始まるかということははっきりしていない。ポケットあるいはbare areaと呼ばれる，軟骨と滑膜の移行部から炎症が始まるとの報告があるが，ヒトの場合ははっきりと証明された文献は少ない。この部位には好中球が最初に浸潤してくるという考え方もあるが，これも確かではない。

我々が発症1年未満のRA患者の膝関節の内側，外側，膝蓋上部の滑膜組織を関節鏡で観察しながら採取して検討したところ，特にどの部位で病変が進んでいるという所見は得られず，むしろ採取部位にかかわらず同時に病変が進行しているという結果を得ている[3]。その組織像は滑膜組織のsublining の毛細血管あるいは小静脈周囲にhuman leukocyte anigen (HLA)-DR陽性の線維芽細胞様細胞（fibroblast like cell：FLC）がまず浸潤し，引き続いてTリンパ球，暫くしてBリンパ球の浸潤が見られるようである[4]。炎症論からいえば急性炎症のstageでは，発症期に滲出と

RA：関節リウマチ，HLA：human leukocyte anigen，FLC：fibroblast like cell（線維芽細胞様細胞）

図3　10週齢のMRL/lマウスの膝関節HE染色像

大腿骨において，成長軟骨，骨髄，骨幹部骨膜の3点に囲まれた部分であるperiphysisには，血管の増生，マクロファージと多核大型細胞の集積が認められる。
HE：ヘマトキシリン-エオジン
（文献10より）

図4　パンヌス周囲の紡錘形細胞の電子顕微鏡像

紡錘形のFLCは多彩な像を示し，滑膜の深部から骨周囲まで浸潤する。この細胞はタンパク合成を示す粗面小胞体や分解酵素を示すリソソームを有する。滑膜深部のFLCとパンヌスのFLCが同一の細胞であるかどうかが問題である。
FLC：線維芽細胞様細胞　（筆者ら提供）

もに好中球が浸潤することは十分考えられる。しかし最近では，RAの炎症がどのような形で始まるかという初期病態の観察のために組織を採取することは，困難になりつつある。

これに対して動物モデルを用いて病態を調べることは可能である。我々がRAなどの自己免疫疾患の動物モデルであるMRL/lマウスを用いて観察した結果，初期はsubchondralにあるossification groove of Ranvier(R zone)から入り込む血管に沿った形でMac-1陽性のマクロファージの浸潤が認められ，そこから炎症が拡大して軟骨に向かって拡がっていることを確認した(図3)[10]。

また，初期には滑膜のsublining にもこのMac-1陽性細胞が出現する[11]。従って，滑膜組織に始まった炎症がポケットあるいはbare areaと呼ばれる部分から軟骨に拡大していくということは，物理的な距離，あるいは物質を透過しやすい有窓性の血管を持つという組織学的特徴からみても妥当性のある意見であると思われるが，今後，精度の高い画像によって観察していくことも可能になると思われる。

滑膜の病変から軟骨の吸収

滑膜の炎症と軟骨の吸収との関係にはまだ解明されていない点もあり，治療による抗炎症効果が上がったと言われながら，骨吸収が十分にコントロールできない問題がここにある。初期病変からみると，RAの病変は滑膜のsublining から始まり，リンパ球やFLCを主体とする炎症性細胞が深部に浸潤し，それが軟骨に及んで肉芽組織（パンヌス）になったのではないかと思われる(図4)。パンヌスでは，リンパ球浸潤とともに血管増生，多彩な細胞像を示すFLCの増殖が特徴であるが，滑膜にみられる炎症性の肉芽組織と軟骨や骨破壊を示す組織が同じ性質を持つものと考えていいかどうかが問題になる(図5)。軟骨，骨での一連の変化については，図6のような因子の関与が考えられる。

軟骨

1．関節液の影響

膝関節の場合，病変のない関節の関節液量は0.5mL程度であり，ヒアルロン酸が多く含まれて

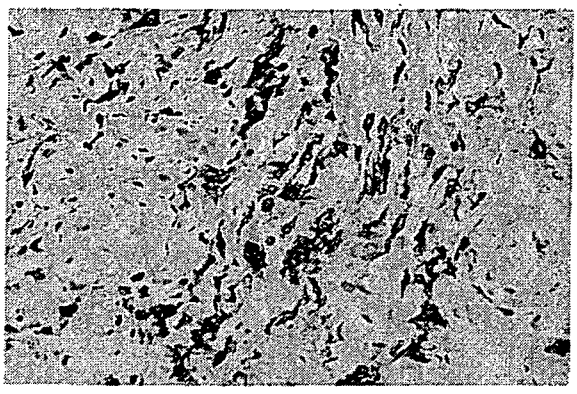

図5　滑膜深部の線維芽細胞様細胞

線維芽細胞様細胞はHLA-DRが陽性となるほかに，細胞によってはCD34，CD68，CD14などが陽性を示し，骨髄のstromal cell由来とも言われている。この写真はMy4（CD14）による免疫染色であるが，線維芽細胞様細胞も陽性になる。

HLA-DR：human leukocyte antigen-DR

（筆者ら提供）

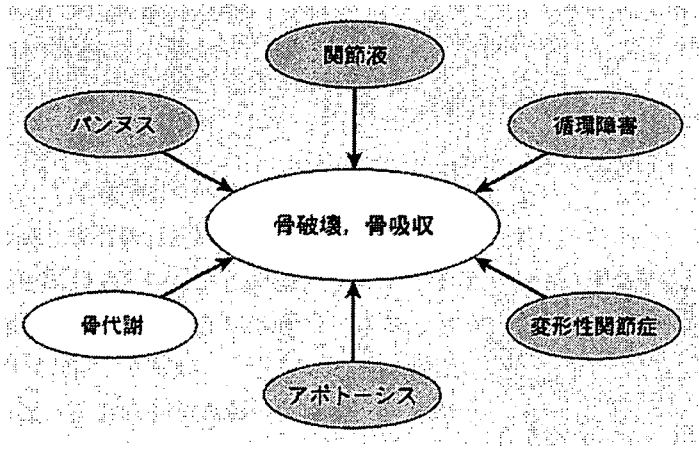

図6　軟骨や骨の変性を惹き起こすさまざまな因子

軟骨や骨に破壊や吸収をもたらす原因には，図のような因子があげられる。これらの因子が同時にあるいは順次作用して破壊が進行する。

（筆者ら提供）

いるため粘性が高く，生物活性はほとんどみられない[12]。それに対してRAの関節液ではヒアルロン酸の分子量が低下し，粘性の低下した滲出液の状態になり，マトリックスメタロプロテアーゼ（MMP）-1，ヒアルロニダーゼをはじめ，多種類のタンパク分解酵素と好中球や滑膜細胞を中心とした細胞が含まれている[7][13]。関節液中のリンパ球は好中球に比べると少ないが，これは好中球の走化性と関節液中の因子との関係による。

しかし，関節液中にあるこれらのタンパク分解酵素が，いつでも活性化されているわけではない。我々の検討では，RA患者から採取した関節液に，実験的にp-aminophenylmercuric acetate（APMA）を入れた状態でゼラチン分解活性がみられるのに対し，OA患者の関節液ではこのような現象はみられない[14]。このことは，RAの関節液に含まれるタンパク分解酵素は通常それほど活性化されておらず，何か急性の症状が発生した場合に酵素の活性化が起こる可能性を示しているが，それが如何なる因子によるかは不明である。

APMA：p-aminophenylmercuric acetate，MMP：マトリックスメタロプロテアーゼ